

PROCEEDINGS OF SPIE

SPIDigitalLibrary.org/conference-proceedings-of-spie

Physical model for the contrast sensitivity of the human eye

Barten, Peter

Peter G. J. Barten, "Physical model for the contrast sensitivity of the human eye," Proc. SPIE 1666, Human Vision, Visual Processing, and Digital Display III, (27 August 1992); doi: 10.1117/12.135956

SPIE.

Event: SPIE/IS&T 1992 Symposium on Electronic Imaging: Science and Technology, 1992, San Jose, CA, United States

PHYSICAL MODEL FOR THE CONTRAST SENSITIVITY OF THE HUMAN EYE

Peter G.J. Barten

*Barten Consultancy
de Huufkes 1, 5511 KC Knegsel, The Netherlands*

Abstract

The contrast sensitivity of the human eye and its dependence on luminance and display size is described on the basis of internal noise in the visual system. With the addition of a global description of the optical MTF of the eye, a complete physical model is presented for the spatial contrast sensitivity function. Calculation results obtained with this model are compared with measurements published in literature.

1. INTRODUCTION

The spatial contrast sensitivity function of the eye plays an important role in the calculation of the required resolution of image display systems, in metrics for image quality, and in algorithms for halftoning and data compression systems. There is, however, no generally agreed standard for this function. A difficulty is, that the contrast sensitivity strongly depends on luminance and display size. In the recently developed SQRI method for the evaluation of visual image quality, a mathematical formula is used which takes both luminance and display size into account^{1,2}. This formula is based on a mathematical approximation of measurement data published in literature. In this paper, we will present a physical model that could serve as a background for such a formula.

The contrast sensitivity of the eye is defined as the reciprocal of the threshold modulation depth or threshold contrast. In our model we assume that this threshold is completely determined by noise. This noise consists of internal noise, generated in the eye and possible external noise, present in the observed image. It is further assumed that the effect of internal noise can be derived from the behavior of the eye at external noise which we described in a previous paper³. With some further assumptions about the effect of lateral inhibition and the optical MTF of the eye, we will present a complete physical model for the spatial contrast sensitivity function of the eye. Measurements published by various authors will be compared with the predictions by this model.

2. EFFECT OF EXTERNAL NOISE ON CONTRAST SENSITIVITY

In the presence of external noise, the threshold contrast of a sinusoidal grating pattern increases from a value M_t without noise to a value M_t' with noise. This value is given by

$$M_t' = \{M_t^2 + (kM_n)^2\}^{0.5} \quad (1)$$

where k is a dimensionless constant, and M_n is the modulation depth of the noise wave components. The constant k in this equation is similar to the constant k introduced by Rose⁴ and also used Schade⁵ for the signal-to-noise ratio of just observable objects. Rose

estimates k to lay in the range of 3 to 7, and Schade uses values ranging from 1.5 to 4.3. The rather high value of k is a kind of safety measure of the visual system to protect itself against false alarm. For the sinusoidal grating patterns considered here, we found values in the range of 2.6 to 5.2 from an evaluation of published threshold measurements of images with external noise³. The actual value of k depends on the amount of advanced knowledge about the observed pattern and the method to determine the threshold. It appears also to be different for different observers.

As mentioned in our previous paper on external noise³, the modulation depth M_n of the noise wave components can be calculated from the spectral density Φ_n of the noise with the aid of the following equation:

$$M_n = \{2 \Phi_n / (XYT)\}^{0.5} \quad (2)$$

where X, Y and T are the spatial and temporal dimensions of the considered picture. For static pictures, the value of T is equal to the integration time of the eye, which is in the order of 0.1 sec. Next to this limited integration capacity in the temporal domain, the eye also has a limited integration capacity in the spatial domain. This means that the values of X and Y are limited by a maximum angular size over which the eye can integrate the information. Furthermore, it appears that there is also a maximum number of cycles over which the eye can integrate the information. This limit has been reported in the last 20 years by many investigators⁶⁻¹³. Both limits influence the actual values of X and Y in Eq. (2). We found that the effect of this influence on X , and similarly on Y , can be described by the following equation:

$$X = \{(1/X_0^2 + 1/X_e^2 + (u/N_e)^2)^{-0.5} \quad (3)$$

where X_0 is the angular size of the observed picture, X_e is the maximum angular size and N_e is the maximum number of cycles over which the eye can integrate the information, and u is the angular spatial frequency. The formula expresses that the integration angle X is equal to the smallest of three items: object size, maximum integration angle, and visual angle determined by the number of cycles. For the value of

N_e in this equation, numbers ranging from 5 to 25 can be found in the above mentioned literature. The large difference between these numbers is caused by the large effect of particular measuring conditions¹⁴⁻¹⁷. We will use here for N_e a number of 15 cycles, which we found to be a good average. For X_e we will use a value of 12° which we derived from contrast sensitivity measurements by Carlson¹⁸ at large viewing angles.

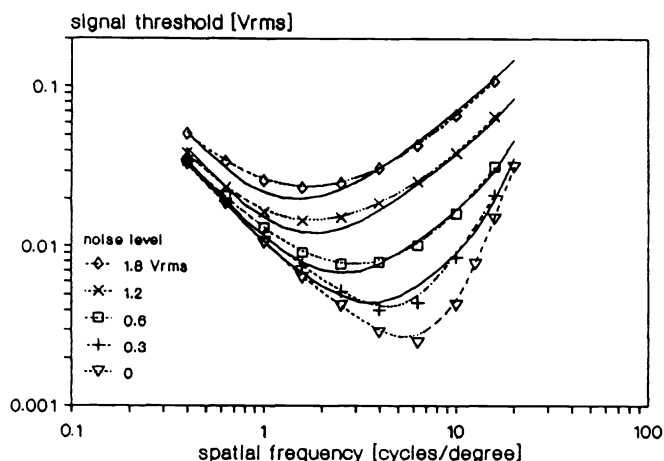


Fig. 1. Increase of threshold contrast at external noise as a function of spatial frequency. Measurements by Pollehn and Roehrig (Ref. 19). The continuous curves were calculated with the given equations.

An example of the increase of the threshold modulation depth in the presence of external noise is given in Fig. 1. This figure shows measured data of this threshold at various amounts of noise for an experiment by Pollehn and Roehrig¹⁹ (data points) together with values calculated with the above given equations (continuous curves). Signal thresholds, as well as noise levels are expressed in V_{rms} . For the calculations the following values

were used: $T = 0.1$ sec, $X_e = 12^\circ$, $N_e = 15$, and $k = 3.1$. For M_t , we used the measured data at zero noise. At high spatial frequencies, the noise curves typically show a slope 1 on the double logarithmic scale of the graph. This slope is caused by the term u/N_e in Eq. (3) expressing the effect of the limited number of cycles.

3. EFFECT OF INTERNAL NOISE ON CONTRAST SENSITIVITY

The above given equations for the effect of external noise on contrast sensitivity can also be applied to internal noise. There are two distinct sources of internal noise: the noise caused by fluctuations of the photon current arriving at the photoreceptors, and neural noise generated in the nerve system. As there is no reason why the eye should react differently on internal noise, as compared to external noise, we can write Eq. (1) in the form:

$$M_t' = k \{ (M_t/k)^2 + M_n^2 \}^{0.5} \quad (4)$$

where M_t/k now represents the modulation depth of the noise wave components caused by internal noise. This means that we assume that the contrast sensitivity of the eye in the absence of external noise is completely determined by internal noise. This also means that for M_t/k a similar equation holds as Eq. (2). However, it must be taken into account that the information received by the eye is filtered by the optical MTF of the eye before reaching the retina. As M_t is measured at the outside of the eye, before this filtering takes place, the noise contribution of the internal noise has to be divided by the optical MTF of the eye. Therefore,

$$M_t/k = \{ 2 \Phi_{int} / (XYT) \}^{0.5} / M_{opt}(u) \quad (5)$$

where Φ_{int} is the spectral density of the internal noise and $M_{opt}(u)$ is the optical MTF of the eye. As the contrast sensitivity is the reciprocal of the modulation threshold, the contrast sensitivity of the eye is

$$1/M_t = 1/k \{ XYT / (2 \Phi_{int}) \}^{0.5} M_{opt}(u) \quad (6)$$

This equation forms the basic concept of our model, together with Eq. (3) for X and Y . We will restrict ourselves here to the spatial contrast sensitivity function valid for static pictures. For these pictures, T is equal to the integration time of the eye. According to Schade⁵, this integration time is 0.1 sec over a very large range of luminance levels. We will use, therefore, this value as a constant value in all our calculations.

The spectral noise density appearing in Eqs. (5) and (6) can be written in the form:

$$\Phi_{int} = \Phi_{ph} + \Phi_{neu} \quad (7)$$

where Φ_{ph} is the spectral density of the photon noise and Φ_{neu} is the spectral density of the noise generated in the neural system, both taken at the entrance of the neural system. This means that when the neural noise is generated in a later stage of the neural system, its contribution has to be translated to the entrance of the system, taking into account possible filter effects.

4. PHOTON NOISE

The effect of photon noise on the contrast sensitivity of the eye was discovered by

de Vries²⁰ in 1943 and further evaluated by Rose⁴ in 1948. The photon noise originates from statistical fluctuations in the photon current. This current depends not only on the luminance of the object but also on the diameter of the iris diaphragm of the eye. Both effects are taken into account in the illuminance I of the eye expressed in trolands (td), which is defined by the following equation:

$$I = \pi/4 d^2 L \quad (8)$$

where d is the diameter of the eye pupil in mm, and L the luminance of the object in cd/m^2 . In this expression d still depends on L . Artificial pupils are sometimes used in experiments in order to keep d fixed. The natural pupil varies from about 2 mm at high light levels to about 8 mm at low light levels. The function $d(-\log L)$ has approximately the shape of a hyperbolic tangent. Published measurements of this function show, however, a large spread. De Groot and Gebhard²¹ made an elaborate survey of these measurements and found as best fitting hyperbolic tangent:

$$d = 4.6 - 2.8 \tanh\{0.4 \log(L/L_0)\} \quad [\text{mm}] \quad (9)$$

where $L_0 = 10^{-0.3} \text{ mL} = 1.6 \text{ cd/m}^2$. We will calculate d with this equation. However, note that in practice deviations of more than 1 mm from the calculated value can occur because of spread between observers and differences in measurement conditions.

If the illuminance I in trolands is known, the photon flux J passing through the cornea can be calculated with the equation

$$J = p I \quad (10)$$

where p is a numerical constant. The value of this constant can be derived from basic photometric and physical quantities²². For monochromatic light the result is:

$$p = 0.6270 \lambda / V(\lambda) \text{ photons}/(\text{td sec arcmin}^2) \quad (11)$$

where λ is the wavelength in nm, and $V(\lambda)$ is the relative spectral sensitivity for this wavelength. For non-monochromatic light, the situation is different. In this case a weighted average has to be calculated with

$$p = 0.6270 \frac{\int P(\lambda) V(\lambda) \lambda d\lambda}{\int P(\lambda) V(\lambda) d\lambda} \text{ photons}/(\text{td sec arcmin}^2) \quad (12)$$

where $P(\lambda)$ is the spectral energy distribution of the light source. For white light of standard illuminant A (color temperature 2854°K), one obtains

$$p = 357 \text{ photons}/(\text{td sec arcmin}^2)$$

These formulae hold for photopic conditions (daylight vision), where the cones act as photoreceptors. At light levels below 0.01 cd/m^2 human vision changes from the photopic to the scotopic condition (night vision), where the rods act as photoreceptors. For scotopic vision, the numerical constant 0.6270 has to be replaced by 0.2442 and the $V(\lambda)$ values for scotopic vision have to be used²³. Most of the measurements that will be discussed here were performed under photopic viewing conditions. Therefore, we will assume this condition in our calculations.

Not all photons that enter the eye generate an excitation of the photoreceptors in the

retina. According to van Meeteren²², the transmission of the ocular media is about 75% to 80%. In the fovea, about 30% of the remaining light falls in the space between the receptors. The receptors themselves absorb about 60% of the incident light and the excitation efficiency of the receptors is also about 60%. This gives a total quantum efficiency of about 20%. In practice, however, much lower values are found: in the order of a few percent or less.

If the total quantum efficiency is η , the photon current that generates an excitation of the nerves is ηJ . According to statistical rules, the spectral density of the noise caused by the fluctuations of this current is

$$\Phi_{ph} = 1/(\eta J) \quad (13)$$

The presence of this noise causes that the contrast sensitivity at low light levels is proportional to the square root of the luminance according to the de Vries-Rose law.

5. NEURAL NOISE AND LATERAL INHIBITION

For the noise generated in the neural system, we must assume that it is not completely white (= independent of spatial frequency), but that its spectral density increases below a certain spatial frequency. This assumption is necessary in order to obtain the well known attenuation of the contrast sensitivity at low spatial frequencies resulting in an about linear increase with spatial frequency at the low frequency side of the curve. We found that this characteristic behavior can be obtained by assuming that

$$\Phi_{neu} = \Phi_0 / \{1 - \exp(-u^2/u_0^2)\} \quad (14)$$

where Φ_0 is the noise density at high spatial frequencies and u_0 is the spatial frequency below which the attenuation of the contrast sensitivity takes place. This frequency is about 8 cycles/degree. In this equation, Φ_0 represents the real neural noise and the denominator represents the effect of a filtering process in an early stage of the neural system.

It is very likely that this filtering is caused by lateral inhibition in the ganglion cells which attenuates the low spatial frequencies of the incoming signals²⁴⁻²⁶. As is generally assumed, the lateral inhibition consists of the subtraction of a spatially low pass filtered signal from the original signal. If the MTF of the low pass filter is $F(u)$, the MTF of the inhibition process can be characterized by $1-F(u)$. To calculate the effect of the neural noise at the entrance of the neural system, this noise has to be divided by the square of the filter MTF. This means that Eq. (14) should have the form:

$$\Phi_{neu} = \Phi_0 / \{1 - F(u)\}^2 \quad (15)$$

Comparing Eqs. (14) and (15) gives

$$F(u) = 1 - \{1 - \exp(-u^2/u_0^2)\}^{0.5} \quad (16)$$

Assuming circular symmetry, the point-spread function $f(r)$ of the low pass inhibition filter that gives such a filtering can be found by a Hankel transform of $F(u)$. However, Eq. (16) is not aiming to give an absolutely exact description of the filter behavior. Therefore, the solution of the Hankel transformation is not unique. This means that there are many possible point-spread functions with different shapes that all have approximately the filter characteristic given by Eq. (16). There is, however, biological

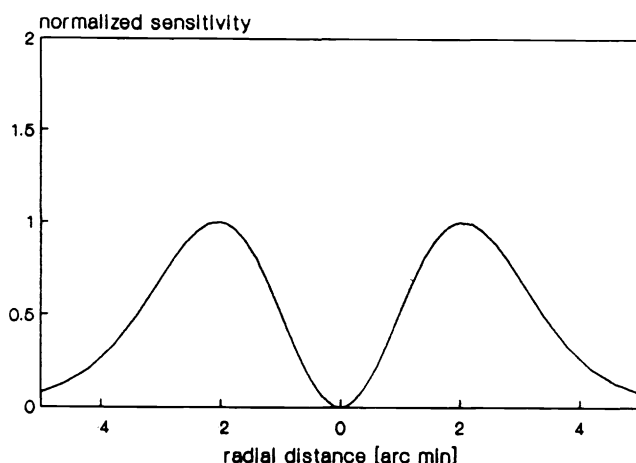


Fig. 2. Point-spread function of the annular inhibition filter applied in our model.

evidence, based on measurements of the electrical response of ganglion cells, that the inhibition filter has an annular shape²⁶. Therefore, we have looked for a solution of the Hankel transformation with an annular shape. The result is given in Fig. 2. The MTF of this point-spread function very closely approximates Eq. (16) with $u_0 = 8$ cycles/degree. The maximum of the function lays on a circle with a radius of 2 arc minutes. This is in good agreement with the results of psycho-physical measurements by Blommaert and Roufs²⁷ of the point-spread function of the eye.

In literature, it is often assumed that the size of the inhibition filter depends on luminance^{24,25}. In our model, we assume that the size and shape of the inhibition filter is independent from luminance.

Combining Eqs. (10), (13) and (15) yields for the total internal noise:

$$\Phi_{int} = 1/(\eta p I) + \Phi_0 / \{1 - F(u)\}^2 \quad (17)$$

The quantity Φ_0 in this equation sets a limit to the contrast sensitivity at high luminance levels. For Φ_0 we found a value of about 3×10^{-8} sec deg². With a cone density of 20,000 cones/deg² in the central fovea and an integration time of 0.1 sec, this would correspond with a statistical fluctuation σ of 8% per cone. If 100 cones would be connected with one nerve fiber leading to the cortex, this would correspond with a fluctuation of 0.8% per nerve line. This seems to be a reasonable figure for a biological system. It means that the neural noise could just be explained by small dissimilarities between the nerve lines. The fluctuation per nerve line would then correspond with a difference of one puls per 0.1 sec in a regular puls train of 1300 pulses/sec.

It would also be possible that the saturation of the contrast sensitivity at high luminance levels is caused by saturation of the signal generation in the cones or by the signal transmission capacity of the nerve fibers. To our opinion, this is not very likely. It would mean that the real neural noise is still lower than the value given above, which seems already to be low. However, if the limit set by one of these factors is indeed lower than the noise limit of the neural system, it would not affect our model, but only lead to an additional term in Eq. (17) and modify the quantitative values of Φ_0 and the inhibition filter.

6. OPTICAL MTF OF THE EYE

In our model, the high frequency decay of the contrast sensitivity function is caused partly by the effect of the limited amount of integration cycles and partly by the optical MTF of the eye (see Fig. 3). This is in agreement with investigation results reported by Banks, Geisler and Bennet²⁸. In our definition the optical MTF includes the optical behavior of the eye lens (mainly spherical aberration and chromatic aberration), straylight from the optical media, diffusion in the retina, and also the discrete structure of the receptor elements. On the basis of the central limit theorem, we assume that the total

effect of these contributions can be described by a Gaussian MTF:

$$M_{opt}(u) = \exp(-\pi^2 \sigma^2 u^2) \quad (18)$$

where σ is the radial standard deviation of the optical point-spread function resulting from the convolution of the various contributions. Even if this point-spread function has not a Gaussian shape, Eq. (18) still gives a good approximation of the actual MTF.

The value of σ depends on the pupil diameter. At large pupil sizes, the value of σ increases with the third power of the pupil diameter because of the spherical aberration of the eye lens. Therefore, we assume that

$$\sigma = \sqrt{\sigma_0^2 + (C_{sph} d^3)^2} \quad (19)$$

where σ_0 is the value of σ at small pupil sizes and C_{sph} is a constant describing the spherical aberration effect. This formula is not valid for (artificial) pupil sizes below 1.5 mm, where the resolution is limited by diffraction. From data of the light distribution on the retina at various pupil sizes given by Vos et al.²⁹, it can be derived that σ_0 is about 1 arc min and C_{sph} is about 0.006 arc min/mm³. We expect that σ_0 will differ between subjects and we will, therefore, adapt this value to the individual measurements, but we also expect that the value of C_{sph} will not differ very much between different observers. Therefore, we will use the value of 0.006 arc min/mm³ as a fixed constant in our calculations.

According to our definition of the optical MTF, also the effect of the discrete structure of the photoreceptors in the retina has to be included in the value of σ_0 . However, from the adaptation of the calculations to the contrast sensitivity measurements, it appeared that the value of $2\sigma_0$ (equivalent disk diameter) was in the range of 1.2 to 1.8 arc min (see table II). This is large compared to the center-to-center distance of the cones in the fovea, which is about 0.5 arc min. This means that for photopic vision, the effect of the discrete structure of the retina on the value of σ_0 may be neglected.

7. TOTAL MODEL

The equations given in the preceding sections lead to the following formula for the contrast sensitivity function:

$$1/M_t = 1/k \sqrt{T/2} \{ [(1/(npI) + \Phi_0 / (1-F(u))^2) \{ (1/X_o^2 + 1/X_e^2 + (u/N_e)^2) \}]^{-0.5} M_{opt}(u) \} \quad (20)$$

for the simple case that the X and Y dimensions of the object are equal. In this equation, the illumination I has to be calculated with Eqs. (8) and (9), $F(u)$ with Eq. (16), and $M_{opt}(u)$ with Eqs. (18) and (19).

The main characteristics of our model are illustrated in Fig. 3, where the effects of neural noise, lateral inhibition, limited number of cycles, optical MTF, and photon noise on the contrast sensitivity function are schematically indicated. The effect of the viewing angle has not been indicated in this figure. This effect will be shown in Fig. 11.

In the following section we will compare the contrast sensitivity calculated with our model with measurements made by various authors. The model contains 9 constants. At the comparison, 6 of these constants will be kept fixed, and 3 will be adapted to the measurements. The fixed constants and their values are given in table I. Sometimes a better agreement with the measurements could be obtained by also adapting one of these

fixed constants. But this was not done, in order to enable a better mutual comparison of the calculated data.

The adapted constants are: the threshold constant k , the quantum efficiency η , and the constant σ_0 for the optical point-spread function of the eye. The values of the adapted constants are listed in table II, together with the values of p (number of photons per troland) calculated with Eqs. (11) or (12).

TABLE I

Fixed constants

T	$= 0.1 \text{ sec}$
X_e	$= 12^\circ$
N_e	$= 15 \text{ cycles}$
Φ_0	$= 3 \times 10^{-8} \text{ sec deg}^2$
u_0	$= 8 \text{ cycles/deg}$
C_{sph}	$= 0.006 \text{ arcmin/mm}^3$

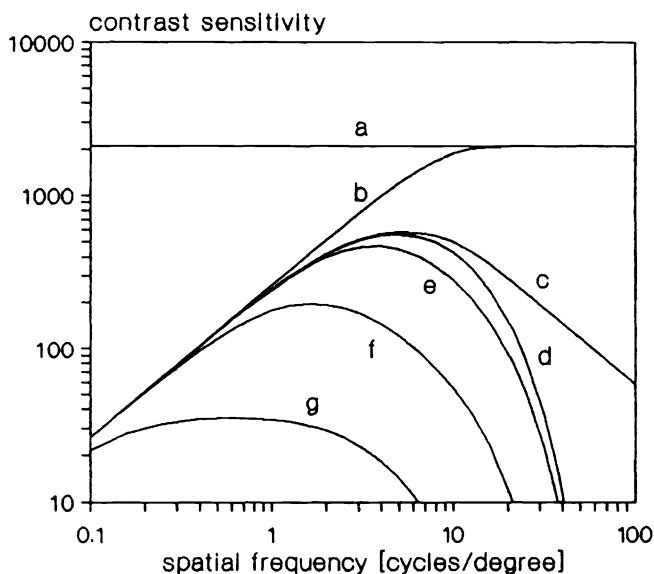


Fig. 3. Effects of various parameters on the contrast sensitivity function: neural noise (a), lateral inhibition (b), limited number of cycles (c), optical MTF (d), and photon noise (e, f, and g).

TABLE II

Adapted values of k , η , and σ_0 , and calculated values of p

<u>author</u>	<u>year</u>	<u>lumin.</u> [cd/m ²]	<u>size</u> [degr]	<u>p</u> [[*])]	<u>k</u>	<u>η</u> [%]	<u>σ_0</u> [arcmin]
DePalma et al. ²⁸	1962	68-1028	6	357	2.7	0.5	0.74
Patel ²⁹	1966	1-300	2	339	3.5	2	0.74
van Nes et al. ³⁰	1967	3×10^{-5} -300	6.1	400	2.8	10	0.60
Campbell et al. ³¹	1968	500	10	342	4.7	2	0.82
Watanabe et al. ³²	1968	34	16.4	342	2.6	4	0.78
van Meeteren et al. ³³	1972	10^{-4} -10	13.7	357	4.0	4	0.84
Virsu et al. ¹⁰	1979	10	var.	342	3.4	1.5	0.63
Carlson ¹⁸	1982	108	0.5-60	342	3.4	3	1.70

^{*}) photons/(td sec arcmin²)

8. COMPARISON WITH MEASUREMENTS

8.1 Measurements made by DePalma and Lowry (1962)

DePalma and Lowry³⁰ measured the contrast sensitivity function at two different luminances: 20 and 300 ftL (68 and 1028 cd/m²). The test object was a vertically oriented

transparent grating illuminated by a variable luminance and combined with a veiling luminance to obtain a variable contrast. The color temperature of the illumination was 2850° K. The threshold contrast was adjusted by the observer, who looked at the test object with both eyes and without an artificial pupil. The measurements at the given luminances were made at a viewing angle of 6° and a viewing distance of 35 in. (89 cm).

Measurements and calculations are shown in Fig. 4. From the figure, it can be seen that the measurements are well described by the calculations, although the measured values for the two luminances merge somewhat quicker at low spatial frequencies than the calculated curves.

8.2 Measurements made by Patel (1966)

Patel³¹ measured the contrast sensitivity function at four different luminance levels ranging from 3 td to 1000 td. The test object was a vertically oriented grating pattern generated on the screen of an oscilloscope tube provided with a green phosphor (P31). The luminance of the patterns was adjusted by the use of appropriate filters. The threshold contrast was adjusted by the observer, who looked at the test object with one eye through an artificial pupil of 2 mm. The viewing angle was 2° and the viewing distance was 1 m. Measurements of only one subject: a male student between the age of 20 and 25, whose results were considered to be "typical".

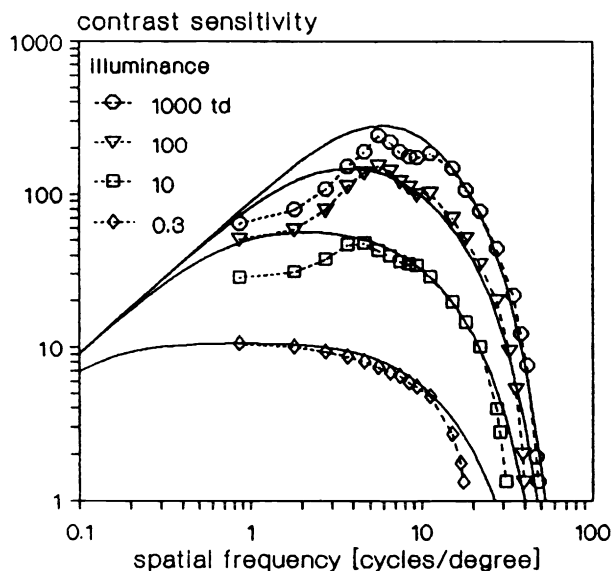


Fig. 5. Contrast sensitivity function measured by Patel (Ref. 31) at four different luminance levels. The continuous curves were calculated with our model.

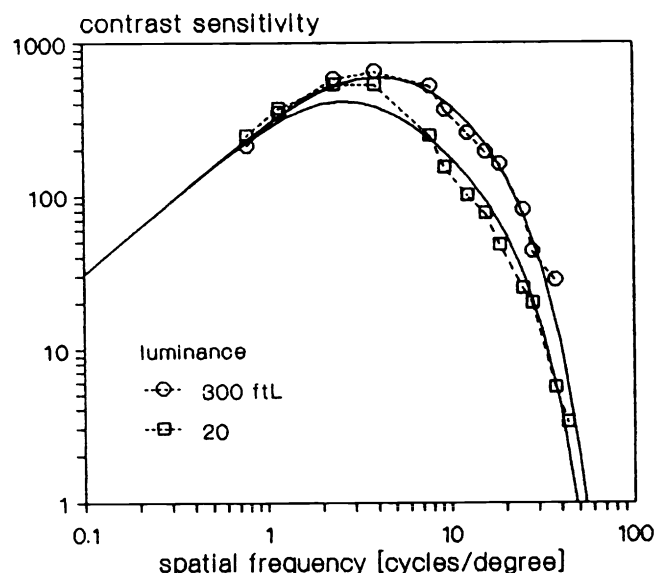


Fig. 4. Contrast sensitivity function measured by DePalma and Lowry (Ref. 30) at two different luminances. The continuous curves were calculated with our model.

Measurements and calculations are shown in Fig. 5. The measurements at 10, 100, and 1000 td generally agree with the calculations, except for a severe dip at about 2 cycles/deg. Such a dip was not found in the other measurements discussed here, so that it has to be assumed that it is caused by some particular measurement condition. This possibility was already mentioned by the authors themselves. An other difference between measurements and calculations is the fact that the measured data for 3 td do not correspond with the calculations for 3 td, but with the calculations for 0.3 td. The value of 3 td mentioned in the paper is clearly an error. Therefore, we assigned a value of 0.3 td to these data in Fig. 5.

8.3 Measurements made by van Nes and Bouman (1967)

Van Nes and Bouman³² made similar measurements, but their measurements extended over a luminance range of six decades and were made at a larger viewing angle and with monochromatic light. The test object was a vertically oriented transparent grating illuminated by a variable luminance and combined with a veiling luminance to obtain a variable contrast. The surrounding field was completely dark. The measurements were made with green light of 525 nm wavelength. The threshold contrast was adjusted in steps by the observer, who looked at the test object with one eye through an optical system with an artificial pupil of 2 mm. The angular size of the test object was 4.5° in horizontal direction and 8.25° in vertical direction. The first author was the observer.

Measurements and calculations are shown in Fig. 6. For the measurement data, the average of sub-threshold value and supra-threshold value was used. The agreement between measurements and calculations over the large range of luminance levels of this experiment is very good, except for a deviation at the left-hand top side of the graph, where the calculations predict a higher asymptotic value. This could have easily been corrected by using a somewhat higher value for u_0 in the calculations. This was, however, not done in order not to disturb the agreement with other measurements. It should further be remarked that not only the vertical position of the calculated curves agrees with the measurements, but also their changing shape at variation of luminance. Only the two lowest curves show some deviations. They are, however, situated in the area of scotopic vision, whereas photopic conditions were assumed in the calculations. The steeper high frequency decay of these curves is probably caused by the larger center-to-center distance of the rods as compared to that of the cones.

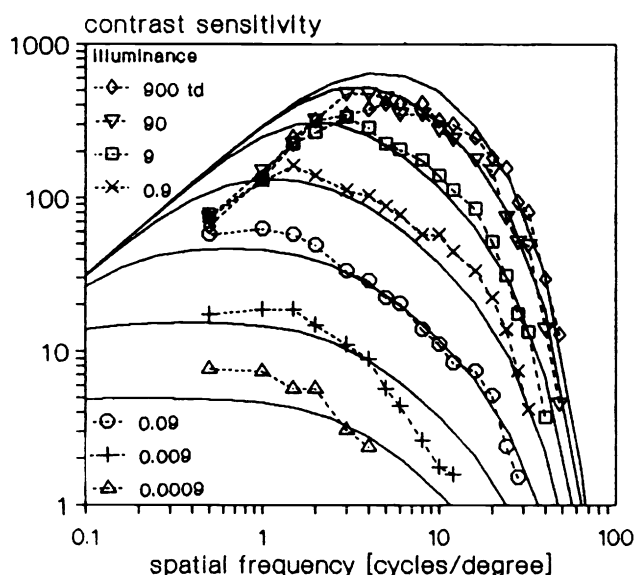


Fig. 6. Contrast sensitivity function measured by van Nes and Bouman (Ref. 32) over a luminance range of six decades. The continuous curves were calculated with our model.

8.4 Measurements made by Campbell and Robson (1968)

Campbell and Robson³³ measured the contrast sensitivity at a constant luminance level of 500 cd/m². The test object was a vertically oriented grating pattern generated on the screen of a monochrome CRT, provided with a white phosphor (P4). The modulating voltage was switched on and off at a rate of 0.5 cycles/sec. We assume here that this rate is still sufficiently low to consider the presentation as static. The contrast was adjusted by the observer until the grating was barely detectable. Either five or ten observations were made for each threshold determination. The observer looked at the test object with one eye through an artificial pupil of 2.5 mm. Measurements at lower spatial frequencies were made with a viewing angle of 10° x 10° and a viewing distance of 57 cm, whereas measurements at higher spatial frequencies were made with a viewing angle of 2° x 2° and a viewing distance of 285 cm. The authors served as subjects. We will use here the measurement data of the second author.

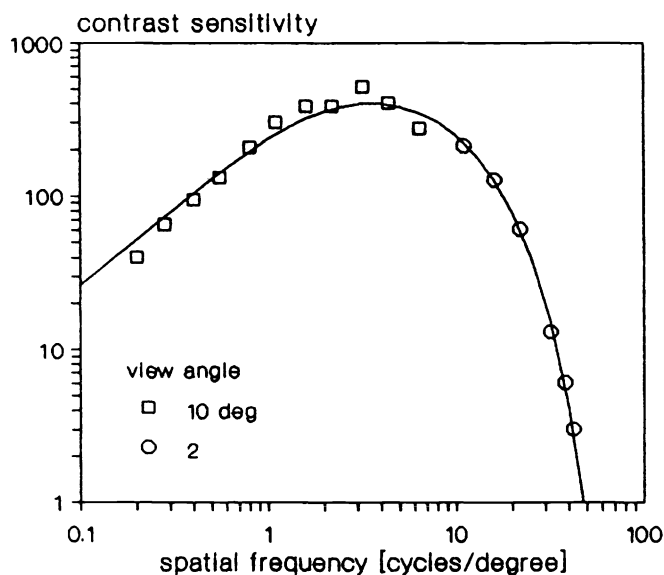


Fig. 7. Contrast sensitivity function measured by Campbell et al. (Ref. 33) at a luminance of 500 cd/m^2 . The continuous curve was calculated with our model.

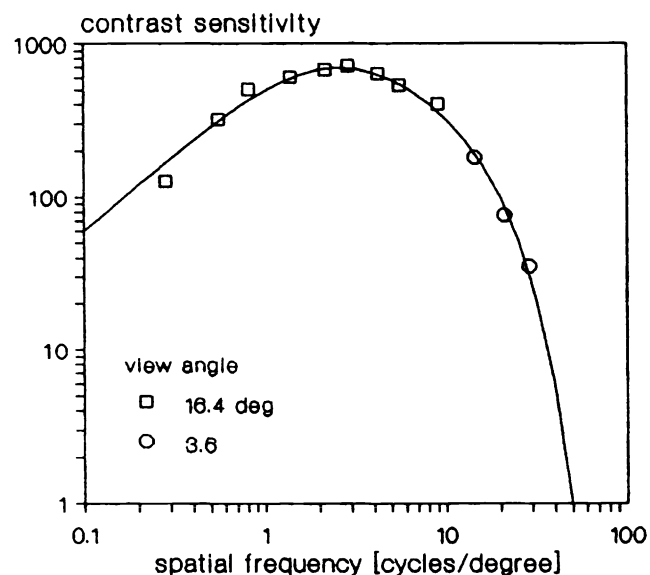


Fig. 8. Contrast sensitivity function measured by Watanabe et al. (Ref. 34) at a luminance of 34 cd/m^2 . The continuous curve was calculated with our model.

Measurements and calculations for a viewing angle of 10° are shown in Fig. 7. The measured data for 10° were completed by adding 2° data for the six highest spatial frequencies. This addition is justified, because calculations showed that there is no difference in contrast sensitivity between both viewing angles at these high spatial frequencies. The measurements show an excellent agreement with the calculations. The very good agreement at high spatial frequencies confirms the validity of the assumption of a Gaussian shape for the optical MTF in combination with the $1/u$ decay caused by the limited amount of cycles.

8.5 Measurements made by Watanabe et al. (1968)

Watanabe et al.³⁴ measured the contrast sensitivity at a constant luminance level of 10 ftL (34 cd/m^2). The test object was a vertically oriented grating pattern generated on the screen of a monochrome television monitor, provided with a white phosphor (P4). The contrast was adjusted by the observer to the point where the grating pattern just disappeared. The observer looked at the test object with both eyes and without an artificial pupil. The size of the test object was 24 cm in horizontal direction and 18 cm in vertical direction. Measurements at lower spatial frequencies were made with a viewing distance of 72 cm , whereas measurements at higher spatial frequencies were made with a viewing distance of 324 cm . This corresponded with an average viewing angle of 16.4° and 3.7° , respectively. Several men and women of ages between 20 and 36 having "normal" vision served as subjects. The data of only one subject were reported.

Measurements and calculations for a viewing angle of 16.4° are shown in Fig. 8. Similarly as for the measurements of Campbell and Robson, the measured data for 16.4° were completed by adding 3.7° data for the highest spatial frequencies. Also in this case, there was no difference in contrast sensitivity between both viewing angles at these spatial frequencies. The measurements show again a very good agreement with the calculations.

8.6 Measurements made by van Meeteren and Vos (1972)

Van Meeteren and Vos³⁵ did similar measurements as van Nes and Bouman, but with white light and a natural pupil, in order to study the contrast sensitivity under conditions closer to natural vision. The luminance was varied over 5 decades from 10^{-4} cd/m² to 10 cd/m². In this luminance range, the pupil size varied from 7 to 5 mm. The test objects consisted of slides with vertical and horizontal grating patterns projected on a white screen at a distance of 3.5 m from the observer. The field size was 17° in horizontal direction and 11° in vertical direction. On this field a uniform luminance was superimposed by a second projector. Contrast and luminance level were varied by inserting neutral density filters and partly also by controlling the lamp currents. The color temperature of the light sources was 2850° K (private communication). Horizontal and vertical gratings were presented in random order to the subject, who had to say "horizontal", "vertical", or "no choice". The transition point of "no choice" answers to correct answers was used as threshold. It was found that this procedure corresponded to 75% correct response in a two-alternative forced-choice method. The measurements were made by two observers. The reported data were averaged over both subjects and both pattern orientations.

Measured and calculated data are shown in Fig. 9. The agreement between measurements and calculations is very good. It should be taken into account that the three lowest curves are situated in the area of scotopic vision, whereas photopic conditions were assumed in the calculations. Similarly as was the case with the measurements of van Nes and Bouman, the steeper high frequency decay of these curves is probably caused by the larger distance between the rods.

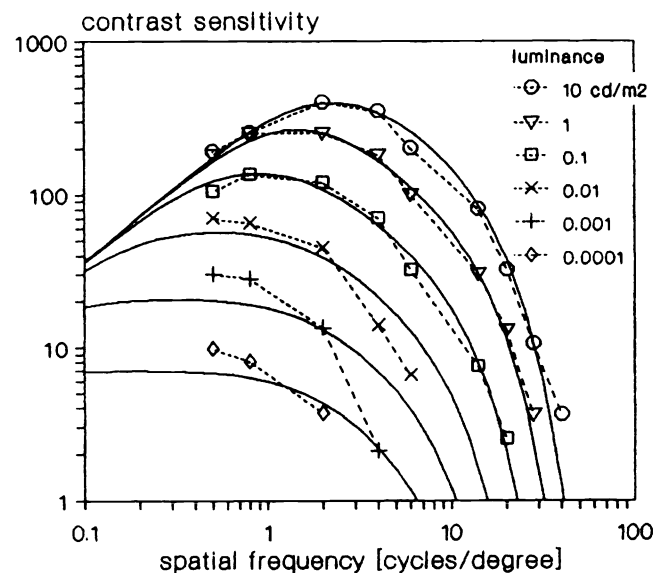


Fig. 9. Contrast sensitivity function measured by van Meeteren and Vos (Ref. 35) over a luminance range of five decades. The continuous curves were calculated with our model.

8.7 Measurements made by Virsu and Rovamo (1979)

Virsu and Rovamo¹⁰ measured the contrast sensitivity as a function of the number of cycles at various spatial frequencies and at a constant luminance level of 10 cd/m². The test object was a vertically oriented grating pattern generated on the screen of a high resolution data display monitor, provided with a white phosphor (P4). The grating patterns had a square size except for a few measurements below 1 cycle. In these cases one full cycle was shown, but the height of the grating was smaller than the width. The surrounds of the gratings had the same luminance as the gratings. The observer looked at the test object with both eyes and without an artificial pupil. The viewing distance was varied in addition to a variation of the grating size, in order to achieve a large variation in angular grating size at all spatial frequencies. Gratings with zero contrast and non-zero contrast were presented in random order. A two-alternative forced-choice method was used to determine the threshold. Seven subjects of ages between 25 and 36 participated in the experiments. The data of only one subject were reported.

Measurements and calculations are shown in Fig. 10. In this figure the contrast sensitivity has been plotted as a function of the number of cycles with the spatial frequency as parameter. The calculated curves agree well with the measurements, especially the curves for 8 and 16 cycles/degree. They clearly demonstrate the saturation at a fixed number of cycles. At low spatial frequencies the agreement is less good.

8.8 Measurements made by Carlson (1982)

Carlson¹⁸ measured the contrast sensitivity function over a range of viewing angles of more than two decades extending from 0.5° to 60°. The luminance level was 34 m^L (108 cd/m²) with a surrounding luminance of 3.4 m^L (10.8 cd/m²). The test objects were vertically oriented square grating patterns. Patterns with angular sizes of 0.5°, 1.0°, 2.3°, and 6.5° were generated on the screen of a monochrome television monitor, whereas patterns with angular sizes of 6.5° and 60° were projected on the screen of an optical projection system. For both systems, the viewing distance was 1.9 m. The results of the 6.5° measurements for the two systems were in good agreement with each other. The observer looked at the test object with both eyes and without an artificial pupil. The threshold was determined by the method of adjustment. The measurements were performed with two subjects. Ten readings were taken at each measurement point for each observer, and the results were averaged.

Measurements and calculations are shown in Fig. 11. The curves give a good example of the dependence of contrast sensitivity on viewing angle. They have asymptotically the same decay at high spatial frequencies. The measurements not only confirm the assumed linear increase of the contrast sensitivity at low spatial frequencies, but also the assumptions about the dependence of contrast sensitivity on viewing angle. As the measurements extend to very large viewing angles, they were used to determine the value of X_e , the maximum angular size over which the eye can integrate the information.

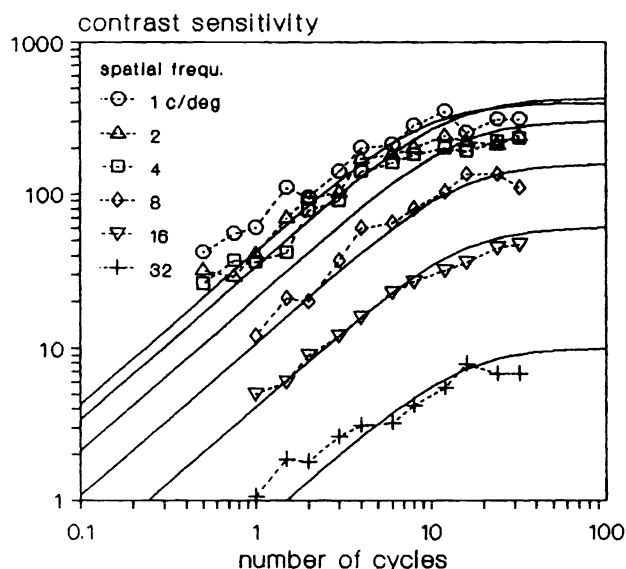


Fig. 10. Contrast sensitivity as a function of the number of cycles measured by Virsu and Rovamo (Ref. 10) at a luminance of 10 cd/m². The continuous curves were calculated with our model.

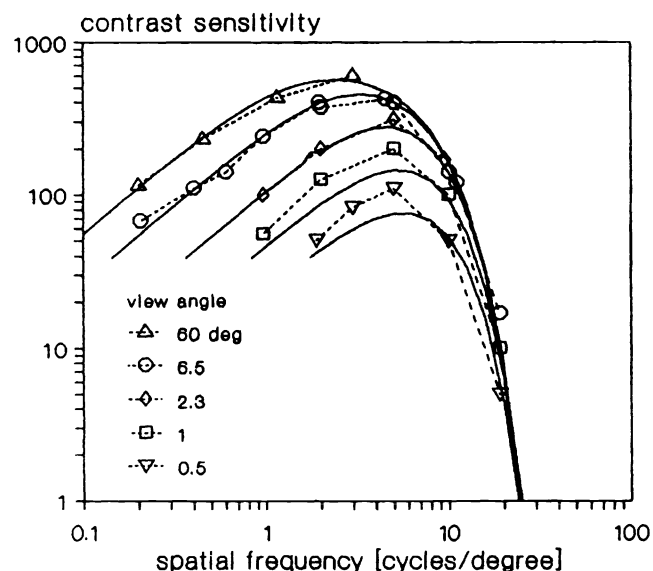


Fig. 11. Contrast sensitivity function measured by Carlson (Ref. 18) at a luminance of 108 cd/m² and a large range of viewing angles. The continuous curves were calculated with our model.

9. DISCUSSION

Concerning the values of the adapted constants given in table II, the following remarks can be made. The spread of the k values is about the same as we found for measurements with external noise³. The spread in the data for the photon efficiency η is much larger than we expected, mainly because of two outliers, and the spread on the values of σ_0 is smaller than we expected, however with one outlier. Typical data for these quantities can be derived by taking the geometric mean of the values mentioned in table II. The result is: $k = 3.3$, $\eta = 2.5 \%$, and $\sigma_0 = 0.8'$. It should, however, be remarked that if we had used a 20% higher value for Φ_0 , all values of k would have been 10% higher and all values of η would have been 20% lower. The choice of the value of Φ_0 was not arbitrarily made, but in such a way that center of the range of k values roughly coincided with that which we found for external noise. It should also be remarked that, if we had taken the integration time of the eye 20% larger, all k values would have increased by 10% without further consequences for the other data. A difference in integration time of the eye between different observers could be responsible for a part of the spread assigned to the k values.

In the analysis, it was implicitly assumed that the various constants did not depend on spatial frequency, luminance, display size, or other parameters that were varied in the experiments. The good agreement between measurements and calculations shows that this assumption was justified. It is in particular amazing that the inhomogeneity of the retina, with its considerable decrease of cone density from the center of the fovea to the periphery, did not cause noticeable deviations at large viewing angles.

10. CONCLUSIONS

A physical model was presented for the spatial contrast sensitivity function of the human eye. The model is based on the assumption that the threshold modulation depth of the eye is completely determined by internal noise, being photon noise and neural noise and that the effect of this noise can be derived from the behavior of the eye at external noise. It was further assumed that the neural noise has partly a spatial $1/f$ character due to lateral inhibition at the entrance of the neural system. For the optical MTF of the eye, a Gaussian function was assumed with a simple dependence on pupil size. In the model, the luminance dependence is taken into account by the photon noise, and the dependence on angular display size is taken into account by a simple rule for the integration capacity of the eye.

The model appears to be in very good agreement with a large number of spatial contrast sensitivity measurements published in literature, covering a large range of luminances and viewing angles.

The model can be used for the calculation of a standard contrast sensitivity function for arbitrary conditions of luminances and display sizes. This could be of great practical advantage for a large number of technical applications.

Although the model gives a good quantitative description of the spatial contrast sensitivity function and a better understanding of the operation of the human visual system, it still leaves many questions unanswered. These could be subject of further investigations. It would also be worth while to try to extend the model into the temporal domain.

11. ACKNOWLEDGEMENT

The author wishes to express his gratitude to Dr. A. van Meeteren of the Institute for Perception TNO, Soesterberg, The Netherlands, and Prof.Dr. J.A.J. Roufs and Prof.Dr. F.L. van Nes of the Institute for Perception Research (IPO) of the University of Eindhoven, The Netherlands, for their advices during this investigation.

REFERENCES

1. P.G.J. Barten, "The square root integral (SQRI): a new metric to describe the effect of various display parameters on perceived image quality," Proc. SPIE, Vol. 1077 (Human Vision, Visual Processing and Digital Display), pp. 73-82, Jan. 1989.
2. P.G.J. Barten, "Evaluation of subjective image quality with the square-root integral method," J. Opt. Soc. Am. A, Vol. 7, No. 10, pp. 2024-2031, Oct. 1990.
3. P.G.J. Barten, "Evaluation of the effect of noise on subjective image quality," Proc. SPIE, Vol. 1453 (Human Vision, Visual Processing and Digital Display II), pp. 2-15, Febr. 1991.
4. A. Rose, "The sensitivity performance of the human eye on an absolute scale," J. Opt. Soc. Am., Vol. 38, No. 2, pp. 196-208, Febr. 1948.
5. O. Schade, "Optical and photoelectric analog of the eye," J. Opt. Soc. Am., Vol. 46, No. 9, pp. 721-739, Sept. 1956.
6. J. Hoekstra, D.P.J. van der Goot, G. van den Brink and F.A. Bilsen, "The influence of the number of cycles upon the visual contrast threshold for spatial sine wave patterns," Vision Res., Vol. 14, No. 6, pp. 365-368, June 1974.
7. J.J. McCann, R.L. Savoy, J.A. Hall Jr and J.J. Scarpetti, "Visibility of continuous luminance gradients," Vision Res., Vol. 14, No. 10, pp. 917-927, Oct. 1974.
8. R.L. Savoy and J.J. McCann, "Visibility of low-spatial-frequency sine-wave targets: dependence on the number of cycles," J. Opt. Soc. Am., Vol. 65, No. 3, pp. 343-350, March 1975.
9. E.R. Howell and R.F. Hess, "The functional area for summation to threshold for sinusoidal gratings," Vision Res., Vol. 18, No. 4, pp. 369-374, April 1978.
10. V. Virsu and J. Rovamo, "Visual resolution, contrast sensitivity, and the cortical magnification factor," Exp. Brain Res., Vol. 37, No. 3, pp. 475-494, 1979.
11. J.G. Robson and N. Graham, "Probability summation and regional variation in contrast sensitivity across the visual field," Vision Res., Vol. 21, No. 3, pp. 409-418, March 1981.
12. J.H.T. Jamar and J.J. Koenderink, "Sine-wave gratings: scale invariance and spatial integration at suprathreshold contrast," Vision Res., Vol. 23, No. 8, pp. 805-810, Aug. 1983.
13. S. Takahashi and Y. Ejima, "Dependence of apparent contrast for a sinusoidal grating on stimulus size," J. Opt. Soc. Am. A, Vol. 1, No. 12, pp. 1197-1201, Dec. 1984.
14. O. Estevez and C.R. Cavonius, "Low-frequency attenuation in the detection of gratings; sorting out the artefacts," Vision Res., Vol. 16, No. 5, pp. 497-500, May 1975.
15. J.J. McCann, R.L. Savoy and J.A. Hall Jr, "Visibility of low-frequency sine-wave targets: dependence on number of cycles and surround parameters," Vision Res., Vol. 18, No. 7, pp. 891-894, July 1978.
16. J.J. McCann and J.A. Hall Jr, "Effects of average-luminance surrounds on the visibility of sine-wave gratings," J. Opt. Soc. Am., Vol. 70, No. 2, pp. 212-219, Febr. 1980.
17. G.J. van der Wildt and R.G. Waarts, "Contrast detection and its dependence on the presence of edges and lines in the stimulus field," Vision Res., Vol. 23, No. 8, pp. 821-830, Aug. 1983.

18. C.R. Carlson, "Sine-wave threshold contrast-sensitivity function: dependence on display size," *RCA Review*, Vol. 43, pp. 675-683, Dec. 1982.
19. H. Pollehn and H. Roehrig, "Effects of noise on the modulation transfer function of the visual channel," *J. Opt. Soc. Am.*, Vol. 60, No. 6, pp. 842-848, June 1970.
20. H. de Vries, "The quantum character of light and its bearing upon threshold of vision, the differential sensitivity and visual acuity of the eye," *Physica*, Vol. 10, pp. 553-564, July 1943.
21. S.G. de Groot and J.W. Gebhard, "Pupil size determined by adapting luminance," *J. Opt. Soc. Am.*, Vol. 42, No. 7, pp. 492-495, July 1952.
22. A. van Meeteren, "On the detective quantum efficiency of the human eye," *Vision Res.*, Vol. 18, No. 3, pp. 257-267, March 1978.
23. H. Scheibner and E. Baumgardt, "Sur l'emploi en optique physiologique des grandeurs scotopiques," *Vision Res.*, Vol. 7, No. 1, pp. 59-63, Jan. 1967.
24. C. Enroth-Cugell and J.G. Robson, "The contrast sensitivity of retinal ganglion cells of the cat," *J. Physiol.* Vol. 187, pp. 517-552, 1966.
25. A.M. Rohaly and G. Buchsbaum, "Global spatiochromatic mechanism accounting for luminance variations in contrast sensitivity functions," *J. Opt. Soc. Am. A*, Vol. 6, No. 2, pp. 312-317, Febr. 1989.
26. R.A. Young, "Oh say, can you see? The physiology of vision," *Proc. SPIE*, Vol. 1453 (Human Vision, Visual Processing and Digital Display II), pp. 92-123, Febr. 1991.
27. F.J.J. Blommaert and J.A.J. Roufs, "The foveal point spread function as a determinant for detail vision," *Vision Res.*, Vol. 21, No. 8, pp. 1223-1233, Aug. 1981.
28. M.S. Banks, W.S. Geisler and P.J. Bennet, "The physical limits of grating visibility," *Vision Res.*, Vol. 27, No. 11, pp. 1915-1924, Nov. 1987.
29. J.J. Vos, J. Walraven, and A. van Meeteren, "Light profiles of the foveal image of a point source," *Vision Res.*, Vol. 16, No. 2, pp. 215-219, Febr. 1976.
30. J.J. DePalma and E.M. Lowry, "Sine-wave response of the visual system. II. Sine-wave and square-wave sensitivity," *J. Opt. Soc. Am.*, Vol. 52, No. 3, pp. 328-335, March 1962.
31. A.S. Patel, "Spatial resolution by the human visual system. The effect of mean retinal illuminance," *J. Opt. Soc. Am.*, Vol. 56, No. 5, pp. 689-694, May 1966.
32. F.L. van Nes and M.A. Bouman, "Spatial modulation transfer in the human eye," *J. Opt. Soc. Am.*, Vol. 56, No. 5, pp. 689-694, May 1966.
33. F.W. Campbell and J.G. Robson, "Application of Fourier analysis to the visibility of gratings," *J. Physiol.* Vol. 197, pp. 551-566, 1968.
34. A. Watanabe, T. Mori, S. Nagata and K. Hiwatashi, "Spatial sine-wave responses of the human visual system," *Vision Res.*, Vol. 8, No. 9, pp. 1245-1263, Sept. 1968.
35. A. van Meeteren and J.J. Vos, "Resolution and contrast sensitivity at low luminances," *Vision Res.*, Vol. 12, No. 5, pp. 825-833, May 1972.